Journal of Statistical Physics, Vol. 76, Nos. 5/6, 1994

Incommensurate–Commensurate Phase Transitions in an Anisotropic Antiferromagnetic Model on Triangular Lattice

Pavol Pajerský[1] and Anton Šurda[1]

Received December 14, 1993; final February 16, 1994

An anisotropic antiferromagnetic model on a triangular lattice with competing interactions is investigated by the cluster transfer-matrix method. A phase diagram with ferrimagnetic, incommensurate, and disordered phases is found. Three order parameters are introduced. At commensurate–incommensurate and incommensurate–disorder phase transition lines two of them change in continuous and one in discontinuous way.

KEY WORDS: Anisotropic antiferromagnetic model; incommensurate phase; Kosterlitz–Thouless phase; cluster transfer-matrix method.

1. INTRODUCTION

The triangular Ising model with antiferromagnetic nearest-neighbor and ferromagnetic next-nearest-neighbor interactions has attracted considerable interest in the last two decades. It was used to describe physical adsorption of gases on graphite[1] and as a simple example of a model with a rich phase diagram with critical lines, tricritical point, and Kosterlitz–Thouless critical phase. Campbell and Schick[1] used a two-site mean-field approximation (Bethe approximation). Their results differ substantially from later calculations of the phase diagram by the Monte Carlo method,[2,3] symmetry considerations,[4] group theory analysis,[5] and the transfer-matrix method.[6] All these works, using finite-size scaling arguments, confirmed a $\sqrt{3} \times \sqrt{3}$ ordered phase for small magnetic field with a line of a second- and first-order phase transition to disordered state and a tricritical point between

[1] Institute of Physics, Slovak Academy of Science, Dúbravská cesta 9, 842 28 Bratislava, Slovakia.

0022-4715/94/0900-1467$07.00/0

them. The second-order phase transition belongs to the universality class of the three-state Potts model. Another continuous critical line was found at zero field and was concluded to belong to the universality class of the two-dimensional XY model with hexagonal anisotropy. The critical exponents are nonuniversal and temperature dependent. The phase is clearly seen when the finite-size behavior of the site–site correlation functions is analyzed, but it was not confirmed by the phenomenological renormalization method. [This phase we shall denote as a Kosterlitz–Thouless (KT) phase.]

Recently, Kitatani and Oguchi[7] investigated a simplified model where an anisotropy was introduced by omitting one of the three next-nearest-neighbor ferromagnetic interactions. It was shown that the phase diagram of the model practically did not change. The existence of the KT phase was concluded only from the scaling behavior of the site–site correlation function in this case, as well.

The anisotropic model was studied by the transfer-matrix method[7] for various strip widths and by Monte Carlo calculations[8] using a coarse-graining procedure. From these calculations, it seems very probable that there exist two temperatures T_{c1} and T_{c2} where the Kosterlitz–Thouless phase transitions take place and the system at all temperatures between them is in a critical state. The existence of two conspicuous temperatures is seen from two peaks in the specific heat as well.

We use the cluster transfer-matrix method—a combination of the transfer-matrix and the mean-field approach—to confirm the existence of a new phase between the ordered and the disordered phases and to show that the predicted KT phase is in fact an incommensurate structure.

2. MODEL AND METHOD

We shall calculate the free energy and the local magnetization of a system of ± 1 spins on a triangular lattice interacting by nearest-neighbor (nn) and next-nearest-neighbor (nnn) interactions by the cluster-matrix method developed by one of us.[9-11] All the nn interactions of the model are equal and antiferromagnetic. One of the ferromagnetic nnn interactions is missing. Let us choose in our triangular two-dimensional lattice zigzag rows in the direction of the missing next-nearest-neighbor interaction (see Fig. 1). As there are no competing interactions in this direction, we expect the presence of only simple commensurate structures along the rows. Anticipating the size of the clusters in the further approximations, we represent the Hamiltonian of the model as a sum of energies of 2×3 clusters.

There are two types of 2×3 clusters with a two-site base on ascending and descending parts of the zigzag row, respectively. Both clusters can be

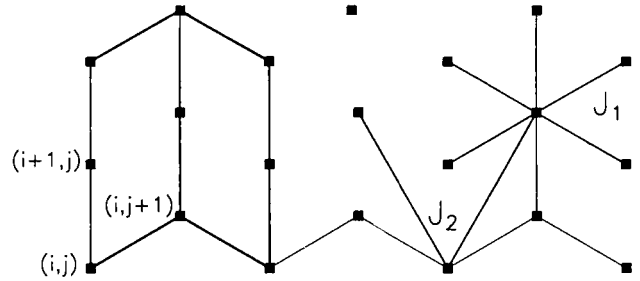

Fig. 1. Anisotropic model on a triangular lattice with two competing interactions: J_1, nn interactions; J_2, nnn interactions. The two six-site clusters are shown by the thick lines and the zigzag row by the thin line.

transformed into each other by mirror reflection with respect to the vertical axis.

Denoting the nearest-neighbor interactions as J_1 and the next-nearest ones as J_2, we have for the energy of the cluster with the ascending base having the left bottom corner at the ith row and the jth column

$$\begin{aligned} G_{i,j} = J_1 \Bigg[& \sigma_{i+1,j} \left(\frac{\sigma_{i,j}}{4} + \frac{\sigma_{i,j+1}}{2} + \frac{\sigma_{i+1,j+1}}{3} + \frac{\sigma_{i+2,j}}{4} \right) \\ & + \sigma_{i+1,j+1} \left(\frac{\sigma_{i,j+1}}{4} + \frac{\sigma_{i+2,j+1}}{4} + \frac{\sigma_{i+2,j}}{2} \right) \\ & + \frac{\sigma_{i+2,j}\sigma_{i+2,j+1}}{3} + \frac{\sigma_{i,j}\sigma_{i,j+1}}{3} \Bigg] \\ & + J_2 \left[\frac{\sigma_{i,j}\sigma_{i+1,j+1}}{2} + \frac{\sigma_{i+1,j}\sigma_{i+2,j+1}}{2} + \sigma_{i,j+1}\sigma_{i+2,j} \right] \end{aligned} \tag{1}$$

The expression for the energy of the other cluster is found by interchanging $i \leftrightarrow i+1$ in (1). The terms in (1) are divided by the number of appearances of the particular bond in different clusters.

Then the Hamiltonian of our anisotropic antiferromagnetic model with nn and nnn interactions is simply

$$H = \sum_{i,j} G_{i,j}$$

If in calculation of the partition function

$$Z = \sum_{\{\sigma_i\}} \exp[\beta H(\sigma_i)]$$

the summation is performed consecutively row by row, the problem is equivalent to evaluation of auxiliary functions Ψ_i and numbers λ_i

$$\sum_{S_i} \Psi_i(S_i, S_{i+1})\, T_i(S_i, S_{i+1}, S_{i+2}) = \lambda_i \Psi_{i+1}(S_{i+1}, S_{i+2}) \tag{2}$$

starting from an appropriate function $\Psi_1(S_1, S_2)$.[9] (S_i denotes a row variable $S_i \equiv \{..., \sigma_{i,j}, \sigma_{i,j+1}, \sigma_{i,j+2}, ...\}$ and $T_i(S_i, S_{i+1}, S_{i+2}) = \exp[\beta \sum_{j=-\infty}^{j=+\infty} G_{i,j}]$.)

As S_i consists of an infinite number of site variables $\sigma_{i,j}$ ($j = -\infty, ..., +\infty$), all the values of the auxiliary functions $\Psi_i(S_i)$ cannot be generally found.

Assuming an asymptotic behavior of correlation functions already at distances exceeding the cluster size, we can factorize $\Psi_i(S_i, S_{i+1})$ in the same way as the function $T_i(S_i, S_{i+1}, S_{i+2}) = \prod_{j=-\infty}^{\infty} \exp(G_{i,j})$, i.e.,

$$\Psi_i(S_i, S_{i+1}) \simeq \prod_{j=-\infty}^{\infty} \Psi_{i,j}(s_{i,j}^k) \tag{3}$$

where $s_{i,j}^k$ denotes a set of site variables of a finite two-row cluster

$$s_{i,j}^k = \begin{pmatrix} \sigma_{i+1,j} \cdots \sigma_{i+1,j+k} \\ \sigma_{i,j} \quad \cdots \quad \sigma_{i,j+k} \end{pmatrix}$$

The order of the approximation is given by the size of the cluster. Further, we put $k = 1$, i.e., $\Psi_{i,j}(s_{i,j}^1)$ is defined on a four-site cluster and possesses 16 values.

Substituting (3) into (2), we obtain a relation between known functions $\Psi_{i,j}$ found in the preceding iteration step and the functions $\Psi_{i+1,j}$. Unfortunately, the number of equations (2) is much higher than the number of unknown values of the functions $\Psi_{i+1,j}$. To reduce it, we sum over all sites of the rows $i+1, i+2$ except the sites in the columns $j, ..., j+k$. (Let us denote this infinite set of sites as $M_{i+1}^{j,k}$.) Then the number of equations is equal to the number of values of the unknown functions. We have to find the values of $\Psi_{i+1,j}$ from the equation

$$\sum_{M_{i+1}^{j,k}} \sum_{S_i} \prod_{l=-\infty}^{\infty} \Psi_{i,l}(s_{i,l}^k)\, T_i(S_i, S_{i+1}, S_{i+2}) = \lambda_i \sum_{M_{i+1}^{j,k}} \prod_{l=-\infty}^{\infty} \Psi_{i+1,l}(s_{i+1,l}^k) \tag{4}$$

Let us denote the left-hand side of (4) by $L_{i+1,j}^k$. The functions $\Psi_{i,j}$ and T_i are known and evaluation of $L_{i+1,j}^k$ can be performed again by the tech-

nique of auxiliary functions. Now, because $M_{i+1}^{j,k}$ is one-dimensional, no further approximation is necessary. As we assume the existence of only commensurate structures in the row direction, in the process of iteration, the auxiliary functions will converge to a finite number of their exact values. It is easily seen[11] that $\Psi_{i+1,j}$ is given in terms of $L_{i+1,j}^k$ as

$$\Psi_{i+1,j}(s_{i+1,j}^k) = L_{i+1,j}^k(s_{i+1,j}^k) \Big/ \sum_{\{\sigma_{i+1,j},\sigma_{i+2,j}\}} L_{i+1,j}^k(s_{i+1,j}^k) \tag{5}$$

The solution (5) is not unambiguous. It is possible to insert a product $U_j \cdot U_j^{-1}$ between each two terms $\Psi_{i,j}(s_{i,j}^k)\,\Psi_{i,j+1}(s_{i,j+1}^k)$ in (3), where U_j is an arbitrary function of $s_{i,j+1}^{k-1}$.

There is a direct relation between the structure of the system for different values of interaction constants and the space dependence of the auxiliary functions $\Psi_{i,j}$. In the paramagnetic phase $\Psi_{i,j}$ does not depend on i, in the ferrimagnetic phase $\Psi_{i,j}$ is a periodic function of i with the period of three lattice constants, and in the incommensurate phase its period is a continuous function of interaction constants.

For our model the auxiliary function $\Psi_{i,j}$ is always j-dependent, because we have two kinds of the functions $T_{i,j}$—different for odd and even j. For ferrimagnetic and incommensurate structures the periodicity of $\Psi_{i,j}$ in j is always commensurate and equal to 6.

The free energy of the system is proportional to $\log \prod \lambda_i$. The normalization constant λ_i is, from (4), equal to $\sum L_{i+1,j}^k$, because $\sum \prod \Psi_{i+1,j} = 1$. Using the technique of auxiliary functions, we can again obtain $\sum L_{i+1,j}^k$ as a product of normalization constants. This result is exact because the summation is one-dimensional.

Equation (5) represents a nonlinear mapping of auxiliary functions $\Psi_{i,j}$ on $\Psi_{i+1,j}$. A nonlinear approach to the description of incommensurate structures was previously used by Jensen and Bak.[12] In distinction to our method, they mapped quantities with direct physical meaning—the site magnetizations. The mapping formulas were derived from MFA equations. The change of the subjects of mapping to unphysical quantities in our approach leads to stable fixed orbits, which, together with possibility to increase straightforwardly the order of the approximation, enables us to perform the mapping in high-dimensional parameter space (16 and 64, in the present calculations).

From the knowledge of the functions $\Psi_{i,j}$, it is possible to find the site magnetizations as well. We have

$$\langle \sigma_{i,l} \rangle = \sum_{S_i, S_{i+1}} \prod_j \Psi_{i,j}(s_{i,j}^k)\, \sigma_{i,l} \tilde{\Psi}_{i',j}(s_{i,j}^k) \tag{6}$$

The functions $\Psi_{i,j}$ and $\tilde{\Psi}_{i',j}$ are results of iteration (5) in opposite directions from opposite lattice boundaries, where i and i' are distances from them. If $\langle \sigma_{i,l} \rangle$ is given by (6), then

$$\langle \sigma_{i+1,l} \rangle = \sum_{S_{i+1}, S_{i+2}} \prod_{j} \Psi_{i+1,j}(s^k_{i+1,j})\, \sigma_{i+1,l} \tilde{\Psi}_{i'-1,j}(s^k_{i+1,j})$$

The ferrimagnetic phase is three times degenerate; the lattice structure can appear in three equivalent positions. The actual position of the structure is given by the boundary conditions. If the boundary conditions at opposite edges of the lattice are incompatible with each other, i.e., they give rise to two structures shifted by a lattice vector with respect to each other, the expression

$$F = \log \sum_{S_i, S_{i+1}, S_{i+2}} \prod_{j} \Psi_{i,j} T_i(S_i, S_{i+1}, S_{i+2}) \prod_{k} \Psi_{i'-2,k} \tag{7}$$

is the free energy of the interface between these two phases.

The summation in (7) is performed over the three rows (a period of the structure) and can be done exactly. For longer periods the approximate summation scheme (4) has to be used. The choice of i' in (6) is given by the requirement of minimum of the interface free energy (7). In the incommensurate structures the period cannot be expressed as a multiple of the lattice constant and the interface free energy can be evaluated only approximately.

3. RESULTS AND DISCUSSION

The calculations have shown that the anisotropy antiferromagnetic model with competing nn and nnn interactions on a triangular lattice can be found in one of the phases: ferrimagnetic, paramagnetic, and the incommensurate one lying between them.

The phase diagram of the model is shown in Fig. 2. For zero nnn interactions due to the infinite degeneracy of the ground state, the ordered phases are absent. The ferrimagnetic structure consists of three ferromagnetically ordered sublattices; the magnetization of one of them is opposite to the magnetizations of the other two sublattices. The total magnetization is nonzero and its sign is the sign of the magnetization of the two sublattices. The phase diagram was calculated in the four-site-cluster approximation ($k = 1$). As the phase transition lines changed only slightly for a higher approximation with $k = 2$ (dashed line), all further results are presented in the lower approximation.

The incommensurate phase can be identified with the KT phase of

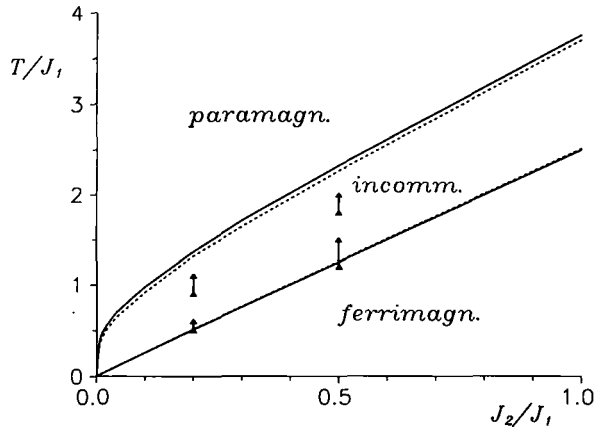

Fig. 2. Phase diagram of the model in two approximations. Solid line, width of the cluster $k=1$; dashed line, $k=2$. The estimates of the phase transition points at $J_2/J_1=0.5$ by Miyashita *et al.*[8] are shown by the thick bars.

Myashita *et al.*[8] The temperature region where our incommensurate phase exists is a little larger than that of the KT phase in that paper.[8] At low temperatures it consists of commensurate $\sqrt{3}\times\sqrt{3}$ domains with domain walls between them. Each two neighboring domains differ by the sign of their magnetizations and the next-nearest-neighboring domains are shifted by one lattice constant with respect to each other (Fig. 3). A detail of the domain wall is shown in Fig. 4.

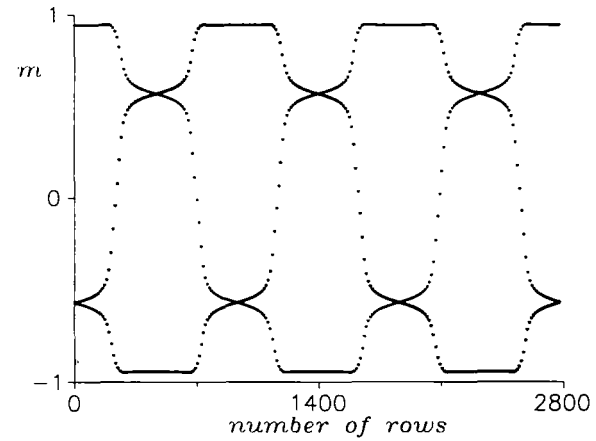

Fig. 3. Site magnetization $m=\langle\sigma\rangle$ as a function of the row number at $T/J_1=1.266$, $J_2/J_1=0.5$.

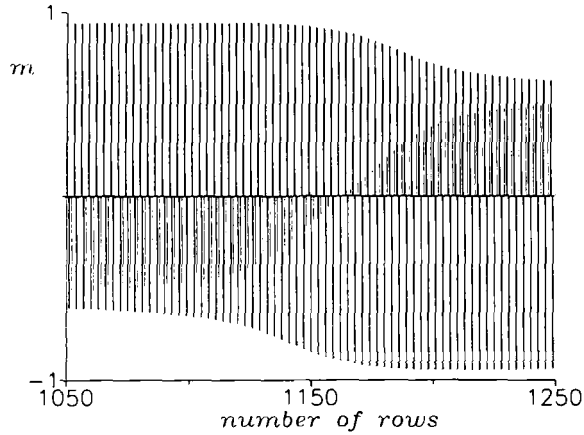

Fig. 4. Detail of the domain wall from Fig. 4.

The spin–spin correlation function decreases exponentially in our approach. The method does not take into account fluctuations of the wall distance at scales exceeding the cluster size. They are responsible for a power-law decrease of the correlation functions with distance in the KT phase.[13-17] Our method treats also dislocations of the walls only partially. Coppersmith *et al.*[18] have shown that an incommensurate structure near a commensurate structure with periodicity p is stable against formation of free dislocations if the inequality $p^2/8 > 1$ is satisfied. In our model $p = 3$.

Let us introduce three order parameters for the description of the incommensurate phase: total magnetization $x_0 = 1/N \sum_i \langle \sigma_{i,j} \rangle$, inverse of the period of the incommensurate structure $x_1 = 1/\lambda$, and local total magnetization $x_2 = [3/N \sum_k (\frac{1}{3} \sum_{\Delta_k} \langle \sigma_{i,j} \rangle)^2]^{1/2}$ (the second sum in x_2 is over a triangular plaquette and the first one over all the plaquettes in the lattice). As shown in Fig. 5, for low temperatures the width of the domains tends to infinity and its inverse—the order parameter x_1—continuously decreases to its value in the $\sqrt{3} \times \sqrt{3}$ structure, that is, equal to zero. The temperature dependence of x_1 near T_1 may be fitted by $x_1 \sim (T - 1.256)^{\alpha}$, where $\alpha \simeq 0.54$, which is close to the Pokrovsky–Talapov value 0.5. The local magnetization x_2 changes also continuously to its commensurate value. On the other hand, the change of the total magnetization x_0 is discontinuous from nonzero value in the commensurate phase to zero in the incommensurate phase.

The discontinuous drop of the total magnetization at T_{c1} probably would be hardly observable in the experiment. The $\sqrt{3} \times \sqrt{3}$ structure near the phase transition line is unstable to the formation of domains of

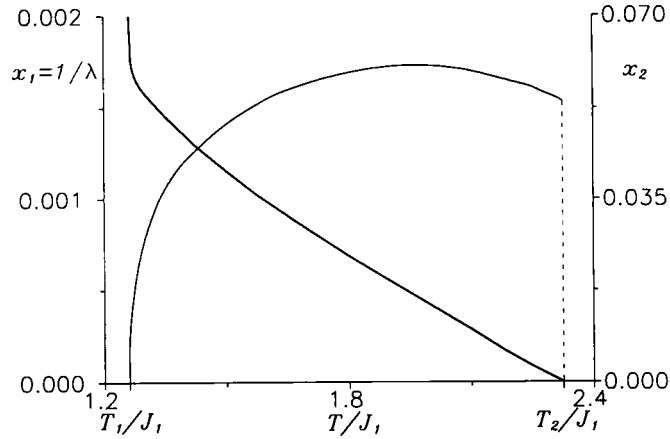

Fig. 5. Temperature dependence of inverse of the wavelength x_1 (thick line) and of the local total magnetization $x_2 = [3/N \sum_k (\frac{1}{3} \sum_{\Delta_k} \langle \sigma_{i,j} \rangle)^2]^{1/2}$ (thin line) of the incommensurate structure for $J_2/J_1 = 0.5$ ($T_1/J_1 = 1.26$, $T_2/J_1 = 2.33$).

opposite sign of magnetization already at weak disturbances of the lattice. A spontaneously formed domain wall can appear only in case of larger distances between impurities than the periodicity of the incommensurate structure. In the lattice with impurities the high-temperature commensurate and the low-temperature incommensurate structures can be only hardly distinguished. We believe that similar considerations could explain a

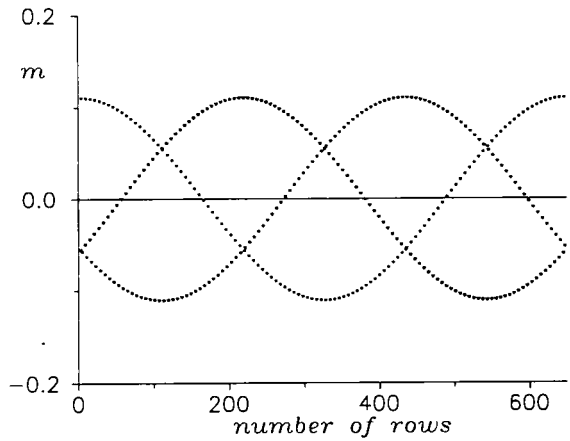

Fig. 6. Site magnetization m as a function of the row number at $T/J_1 = 2.326$, $J_2/J_1 = 0.5$.

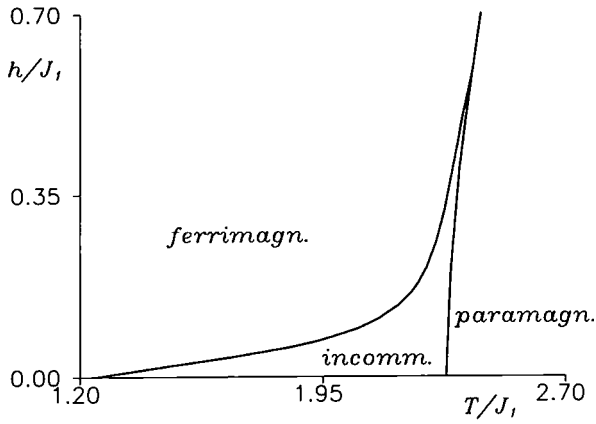

Fig. 7. Phase diagram of the model for small magnetic fields, $J_2/J_1 = 0.5$.

continuous drop of magnetization in Monte Carlo calculations on an ideal lattice.[8] As mentioned above, our method does not describe directly the KT phase. The fluctuations of the wall distances should be included. But even this modification could not restore the nonzero magnetization at the high-temperature side of the I–C phase transition. A different situation is found for the incommensurate–disorder transition line.

With increasing temperature the $\sqrt{3} \times \sqrt{3}$ domains get narrower and finally the space dependence of the magnetization acquires a wavy form (Fig. 6). The inverse of the period x_1 increases and has a maximum slightly before the phase transition line. At the phase transition it drops abruptly to zero value of the paramagnetic structure. On the other hand, the order parameter x_2 goes to the paramagnetic value ($x_2 = 0$) continuously. The total magnetization x_0 is equal to zero in the whole region of the incommensurate structure, but at the I–D phase transition line it is equal to zero also locally. Only the sublattice magnetizations are generally nonzero. The role of impurities should be much less than in the case of long wavelengths at low temperatures and in the experiment a discontinuous behavior should be clearly visible.

At nonzero magnetic field the low-temperature domains with the magnetization opposite to the direction of the magnetic field are suppressed and a clean $\sqrt{3} \times \sqrt{3}$ structure is established. At higher temperatures the structure no longer has a domainlike character and the incommensurate structure persists also for relatively large magnetic fields (Fig. 7). (For comparison, the ferrimagnetic–paramagnetic phase transition at zero temperature occurs at $h/J_1 = 6$.) According to symmetry considerations,[5] the

phase at nonzero magnetic field should not be in the critical state. In our approach, where the pair correlation functions decay with distance exponentially, there are no qualitative differences between the incommensurate structures in zero and nonzero magnetic fields. We believe that also in an experiment a small change of chemical potential would not dramatically change diffraction patterns of adsorbed monolayers with competing nn and nnn interactions.

REFERENCES

1. C. E. Campbell and M. Schick, *Phys. Rev. A* **5**:1919 (1972).
2. B. Mihura and D. P. Landau, *Phys. Rev. Lett.* **38**:977 (1977).
3. D. P. Landau, *Phys. Rev. B* **27**:5604 (1983).
4. S. Alexander, *Phys. Lett.* **54A**:353 (1975).
5. E. Domany, M. Schick, J. S. Walker, and R. B. Griffith, *Phys. B* **18**:2897 (1978).
6. Y. Saito and G. Tabe, *J. Phys. Soc. Jpn.* **54**:2955 (1985).
7. H. Kitatani and T. Oguchi, *J. Phys. Soc. Jpn.* **57**:1344 (1988).
8. S. Miyashita, H. Kitatani, and Y. Kanada, *J. Phys. Soc. Jpn.* **60**:1523 (1991).
9. A. Šurda, *Phys. Rev. B* **43**:908 (1991).
10. A. Šurda, *Physica A* **178**:332 (1991).
11. I. Karasová and A. Šurda, *J. Stat. Phys.* **70**:675 (1993).
12. M. H. Jensen and P. Bak, *Phys. Rev. B* **27**:6853 (1983).
13. J. Vallain and P. Bak, *J. Phys. (Paris)* **42**:657 (1981).
14. J. Villain and P. Bak, *J. Phys. (Paris)* **42**:657 (1981).
15. P. Bak, *Rep. Prog. Phys.* **45**:587 (1982).
16. W. Selke, *Phys. Rep.* **170**:213 (1988).
17. W. Selke, in *Phase Transitions and Critical Phenomena*, Vol. 15, C. Domb and J. L. Lebowitz, eds. (Academic Press, New York, 1992).
18. S. N. Coppersmith, D. S. Fisher, B. I. Halperin, P. A. Lee, and W. E. Brinkmann, *Phys. Rev. Lett.* **46**:549 (1981).